SECTION 4—BIOEFFECTS IN TISSUES WITH GAS BODIES

Several animal models have exhibited thresholds for petechial hemorrhage in lung within the current output of diagnostic ultrasound systems. In addition, thresholds for damage in the mouse intestine due to diagnostic pulses of ultrasound have been explored. The implications for human lung and intestinal exposure to clinical diagnostic ultrasound have not yet been determined. In this section, the data supporting the thresholds of petechial hemorrhage in these organ systems and the morphological observations will be reviewed. The potential mechanical mechanisms of damage to these organs due to diagnostic ultrasound also will be reviewed. Special attention will be given to the occurrence of inertial cavitation both *in vitro* and *in vivo*. The effects of ultrasound parameters, age, and species on the threshold for damage in animal models will be explored.

4.1 MECHANICAL MECHANISMS OF DAMAGE

Although no adverse effects on patients exposed to acoustic output levels typical of currently available diagnostic ultrasound systems have been established to date, several animal models have exhibited a threshold for petechial hemorrhage in lung and intestine. The exact mechanical mechanism that induces this damage in biological tissues has not yet been identified. It appears that gas bodies, either macroscopic or microscopic bubbles, are required in the tissue to elicit the effect (Hartman et al, 1990). It is useful to consider the various physical mechanisms that might lead to tissue damage at the lung surface. Inertial cavitation has been discussed as a possible damage mechanism, though other acoustomechanical effects that act directly on the lung surface could be important. For a discussion of acoustic cavitation and its definition, see Section 2.

For cavitation to play a role in tissue damage, it is important that an isolated gas bubble or nucleation site be available to undergo the energy concentration process, i.e., the bubble growth and implosive collapse, that enables cavitation to induce mechanical damage. However, it seems logical to expect that if some damage to the lung's surface, or visceral pleura, is induced, and this area is continually insonated with ultrasound, some small pockets of gas would be broken away from the lung parenchyma and distributed into the surrounding pleural fluid, where they could act as cavitation nuclei. If cavitation were to occur in the pleural fluid, then the strong mechanical forces associated with cavitation could induce interfacial tissue damage in the visceral pleura.

In the animal studies demonstrating lung damage from exposure to pulses of diagnostic ultrasound, which will be described below, cavitation could be taking place in the gas-rich environment of the capillaries adjacent to the alveoli. The conditions under which bubbles may develop are not well known, although it has been shown that when gas bodies are present they may be driven into oscillation by an acoustic field, with the potential to

produce local stresses on neighboring cells (Flynn, 1964; Apfel, 1982; Vivino et al, 1985; MW Miller et al, 1996; Everbach et al, 1997). In addition, the damage mechanism might involve effects associated with reflection of ultrasound energy at the alveolar epithelial cell membrane interface, which can be considered as an acoustic pressure release surface (Holland et al, 1994). Local reflection of the ultrasound pulses could cause the waveform to strengthen or weaken locally. Relative displacement, or shearing, of the air-tissue interface could also lead to mechanical disruption and damage (Howard and Sturtevant, 1997).

Another plausible mechanism for lung damage is a variation of the well-known spallation effect (Chaussy et al, 1980; Chaussy, 1982; Delius et al, 1988a). When a shock wave strikes the surface of a pressure release interface, such as between water and air, there is a rapid ejection of liquid into the lower density space (the air). This effect occurs because the compressive portion of the sound field cannot be sustained when it strikes the pressure release interface. The rapid release of the pressure into the less dense medium (especially if it is air) can result in large velocities of the interface. Thus, this "spallation" effect could result in mechanical damage to the lung surface, or visceral pleura. Related to spallation is the parametric excitation of surface waves, which can occur over a wide frequency range and at lower amplitudes (Eisenmenger, 1959; Brand and Nyborg, 1965). Ultrasonic humidifiers operate by parametric excitation of surface waves that form jets and droplets (Hansen, 1970). As subsequent acoustic pulses continue to strike a particular location, there would be a gradual fatiguing that would result in damage that is dependent on the strength of the tissues lining that interface. Indeed, the different responses for small animals, which have thin pleura (perhaps weak interfacial tissue), and large animals, which have thick pleura (presumably stronger interfacial tissue), could be explained by this mechanism.

4.2 Evidence of Cavitation *In Vivo* from Lithotripters

It is possible to generate bubbles *in vivo* using the short-duration, high-amplitude acoustic pulses employed by extracorporeal shock wave lithotripters (ESWL). The peak positive pressure for lithotripsy pulses can be as much as 100 MPa and the negative pressure around 20 MPa. Finite amplitude distortion causes high frequencies to appear in high-amplitude diagnostic ultrasound fields. Although ESWL pulses have significant energy at high frequencies, a large portion of the energy is actually in the 100 kHz frequency range, much lower than frequencies in diagnostic scanners. The lower frequency makes cavitation more likely. There is evidence to indicate that collapsing bubbles (such as the one shown in Fig. 4–1) may play a role in stone disruption (Coleman et al, 1987; Delius et al, 1988a; Williams et al, 1989; Vakil and Everbach, 1993; Stonehill et al, 1998). When cavitation due to application of ESWL occurs next to a solid surface, a high-velocity liquid jet may form during collapse generating a sufficient impulse to produce observable damage on metal surfaces (Coleman et al, 1987). The impact is sufficient to pit even solid brass and aluminum plates (Fig. 4–2). Clearly, lithotripsy and diagnostic ultrasound differ in the acoustic power generated and are not comparable in the bioeffects produced. Yet some diagnostic devices produce peak rarefactional pressures greater than 3 MPa, which is in the lower range of lithotripter outputs (Duck et al, 1985, 1987). Interestingly, lung damage and surface petechiae have been noted as side effects of ESWL in clinical cases (Chaussy, 1982). Inertial cavitation was suspected as the cause of this damage, and these results prompted several researchers to study the effects of diagnostic ultrasound exposure on lung parenchyma.

4.3 Ultrasound-Induced Effects on Lung

Lung has proven to be an important tissue to investigate the bioeffects from diagnostic ultrasound. The published literature on the topic is summarized in Table 4–1. The presence of air in the alveolar spaces constitutes a significant source of gas bodies.

Figure 4–1 Collapsing bubble near a boundary. When cavitation is produced near boundaries, a liquid jet may form through the center of a bubble and strike the boundary surface. (Photo courtesy of Lawrence A. Crum, PhD.)

Child et al (1990) measured threshold pressures for hemorrhage in mouse lung exposed to 1 MHz to 4 MHz short-pulse diagnostic ultrasound (i.e., 1 to 10 μs pulse durations). The threshold of damage in murine lung at 4 MHz was established to be 1.4 MPa peak rarefactional pressure, which is below the currently allowed peak output of clinical ultrasound scanners.

Pathological features of this damage included extravasation of blood cells into the alveolar spaces (Penney et al, 1993). Findings suggested that the damage evoked by ultrasound included effects on the microvasculature, or capillaries, only. It was hypothesized that cavitation, originating from gas-filled alveoli, was responsible for the damage. Their data were the first to provide direct evidence that clinically relevant pulsed ultrasound exposures produce deleterious effects in mammalian tissue in the absence of significant heating. Hemorrhagic foci induced by 4 MHz pulsed Doppler ultrasound exposure have also been reported in the monkey (Tarantal and Canfield, 1994). Damage in the monkey lung was of a significantly lesser degree than that in the mouse. Subsequently, thresholds for lung damage from pulsed diagnostic ultrasound have been assessed in neonatal mice (Frizzell et al, 1994; Dalecki et al, 1997a), neonatal pig (Baggs et al, 1996), rat (Holland et al, 1996), rabbit and pig (Zachary and O'Brien, 1995; Dalecki et al, 1997c).

Figure 4–2 Pitting caused by cavitation on a brass plate due to exposure to a lithotripter. (Photo courtesy of Lawrence A. Crum, PhD.)

The photos in Figures 4–3 through 4–6 demonstrate typical hemorrhagic lesions produced by exposure to Doppler ultrasound on the surface of rat and monkey lung. The threshold of ultrasound-induced lung damage is plotted as a function of frequency for the mouse, rat, and pig in Figure 4–7. Note that individual investigators reporting these thresholds (Table 4–1) have utilized different definitions for the onset of damage and have employed different statistical treatments of their data. These threshold data were fit to a model of the form,

$$P_r = m_1 f^{m_2} \qquad (4–1)$$

where P_r is the derated rarefactional threshold pressure, f is the center frequency of the insonifying pulse, and m_1 and m_2 are constants.

The least squares fit is also plotted in Figure 4–7. The least squares values for m_1 and m_2 are 0.63 and 0.54, respectively. Alternatively, a linear regression analysis was performed on $\log(P_r)$ versus $\log(f)$. The slope of the linear regression is equal to m_2 in equation 4–1. The significance of this regression analysis was $P = 0.003$ with $R = 0.611$.

In all of these animal systems, pockets of gas have been proposed to be involved in the production of ultrasonic tissue injury. The majority of this experimental work was conducted with commercial diagnostic ultrasound equipment. In these studies, it was impossible to show categorically that these effects were induced by bubbles because the cavitation-induced bubbles were not observed. Further studies are required to determine the relevance of these findings to the human. In particular, the questions of paramount clinical significance are (1) Does diagnostic ultrasound produce lung damage in humans and, if so, (2) what are the clinical or physiological implications of such damage, and (3) under what exposure conditions does the damage become significant?

4.3.1 Pulse Repetition Frequency and Total Exposure Effects

There is conflicting evidence regarding the effect of pulse repetition frequency (PRF) and total exposure duration (on-time plus quiescent period) on the threshold of lung damage. The exposure conditions for lung hemorrhage in mouse neonates were determined at 10°C with pulsed ultrasound of 10 μs pulse duration (Frizzell et al, 1994). Specimens were

Table 4–1: Summary of Publications on Ultrasound-Induced Lung Damage at Diagnostic Frequencies

Species	Frequency [MHz]	p_r† [MPa]	Derating scheme (dB)	$\frac{p_{r(derated)}}{\sqrt{f}}$	Pulse Duration [μs]	PRF [Hz]	Exposure Duration [s]	Total On-Time [ms]	Reference
Suprathreshold Observations									
Adult mouse	6.0	3.0 5.6	0.4*	1.2 2.2	1	1,250	300	375	O'Brien and Zachary (1997)
Adult mouse	1.1	0.8	1.5	0.6	10	100	180	180	Penney et al (1993)§
Adult rabbit	3.0 6.0	2.7–3.8 2.6–6.6	1.3* 1.8–2.2*	1.3–1.9 0.8–2.2	1	1,250	300	375	O'Brien and Zachary (1997)
Adult pig	2.0	3.3	3.1	1.6	4.0	2,000	600	4,800	Harrison et al (1995)
Adult monkey	4.0	4.2 4.5	1.7*	1.6 1.9	0.7	1,515	300	295	Tarantal and Canfield (1994)
Threshold Observations									
Neonate mouse (Bath temperature = 10°C)	1.0	0.4 1.5	0.0	0.4 1.5	10	100 1,000	180 2.4	164 22	Frizzell et al (1994)
Neonate mouse (Bath temperature = 37°C)	1.2	0.6	0.0	0.6	10	100	180	180	Dalecki et al (1997a)
Juvenile mouse	1.2	0.9	0.4	0.8	10	100	180	180	Dalecki et al (1997a)
Adult mouse	1.2	0.8	1.5	0.7	10	100	180	180	Dalecki et al (1997a)
Adult mouse	1.1	0.5	1.5	0.4	10	100	180	180	Child et al
	1.2	0.8	1.5	0.6	10	100	180	180	(1990)
	1.2	0.8	1.5	0.6	10	10	180	18	
	2.3	0.8	2.0	0.4	10	100	180	180	
	3.5	1.7	2.5	0.7	10	100	180	180	
	3.7	1.4	2.6	0.5	10	100	180	180	
	3.7	1.9	2.6	0.7	1	1,000	180	180	
Adult mouse	1.1	1.1	1.9	0.8	10	17 1,000	180 3	30 30	Raeman et al (1993)§
Adult mouse	2.3	1.0 0.9	1.5	0.6 0.5	10 10	100 100	20 180	20 180	Raeman et al (1996)
Adult rat	4.0	2.5 2.0	1.1* 0.9*	1.1 0.9	1.0 1.0	400 1,250	90 90	36 113	Holland et al (1996)
Neonate pig	2.3	1.1	2.0	0.6	10	100	960	960	Baggs et al (1996)§
Young pig	2.3	1.3	4.0	0.5	10	100	2,160	2,160	Dalecki et al (1997c)
Observations of No Damage Attributable to Ultrasound									
Neonate mouse (Bath temperature = 10°C)	1.2	0.5–2.0	0 dB	0.5–1.9	10	100	180	180	Dalecki et al (1997a)
Adult pig	3.0 6.0	4.1 8.0–8.3	2.0* 3.4*	1.9 2.2–2.3	1	1,250	300	375	O'Brien and Zachary (1997)

*Assumed 0.3 dB/cm-MHz deration scheme.
†Those studies that reported *in situ* values only were extrapolated to obtain water values based on the deration scheme reported.
§The authors were contacted in order to supply some of the data that did not appear in the publication.

Figure 4–3 Arrow marks typical hemorrhagic lesion produced by a 1.5 min exposure to 4 MHz pulsed Doppler ultrasound on the surface of rat lung. The pulse duration was 1.0 μs, and the *in situ* exposure level was 3.2 MPa, corresponding to an MI of 1.6. (Reprinted by permission of Elsevier Science, from Holland CK, et al: Direct evidence of cavitation *in vivo* from diagnostic ultrasound. *Ultrasound Med Biol* 22:917, 1996.)

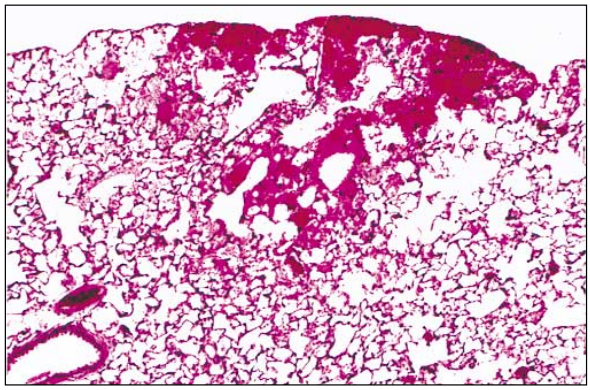

Figure 4–4 Subpleural hemorrhage in rat lung parenchyma exposed to 4 MHz pulsed diagnostic ultrasound. (Reprinted by permission of Elsevier Science, from Holland CK, et al: Direct evidence of cavitation *in vivo* from diagnostic ultrasound. *Ultrasound Med Biol* 22:917, 1996.)

sonicated for 2.4 s at a PRF of 1 kHz and for 180 s at a PRF of 100 Hz. The percentage of specimens exhibiting hemorrhage was determined versus I_{SPPA}, based on a linear extrapolation. The data were fit to a second order polynomial using least squares analysis. Extrapolation of this fit to the value for percentage hemorrhage observed for the sham sonicated specimens (approximately 32%) gave the threshold values for I_{SPPA} of 95 and 4 W/cm^2 for the 2.4 and 180 s exposure durations, respectively. The corresponding values for the peak rarefactional pressure were 1.5 and 0.37 MPa, respectively. The results showed that the threshold exposure conditions for lung hemorrhage are much lower than the conditions for cavitational or other effects reported for tissues that do not contain well-defined gas bodies, confirming the results of Child et al (1990). In addition, the results showed an inverse relation between exposure level and either exposure duration or sound on-time for equivalent damage, suggesting that time is an important parameter associated with lung damage.

In contrast, several studies suggest that the total ultrasound on-time and the exposure duration only weakly influence the threshold for lung hemorrhage (Raeman et al, 1993, 1996). For a constant total on-time of 0.03 s of ultrasound, the damage threshold for a 3 min exposure period (10 μs pulse duration, 17 Hz PRF) was approximately equal to the damage threshold for a 3 s exposure (10 μs pulse duration, 1 kHz PRF) (Raeman et al, 1993). Also, no statistically significant difference in the threshold for murine lung hemorrhage was found at 2.3 MHz (10 μs pulse duration, 100 Hz PRF) for a 20 s exposure duration (on-time of 0.02 s) or 3 min exposure duration (on-time of 0.18 s) (Raeman et al, 1996). Raeman et al (1996) assert that the threshold for lung hemorrhage is relatively insensitive to total exposure time even though the extent and degree of suprathreshold damage increases with time. It is these shorter exposure durations and sound on-times that may be most relevant clinically.

4.3.2 Species-Dependent Effects Due to Pulsed Ultrasound Exposure

There is conflicting evidence regarding the effect of species on the lung damage threshold due to pulsed ultrasound exposure. In a series of studies, the thresholds for lung hemorrhage in mice (Child et al, 1990; Dalecki et al, 1997a) and in swine (Baggs et al, 1996; Dalecki et al, 1997c) have been determined. These authors found that the threshold for lung hemorrhage is not dependent on the species. The extent of the damage relative to the size of the lung, however, was found to be dependent on species. Whereas a suprathreshold exposure in a mouse may damage a large percentage of the lung, the same exposure would produce a localized lesion in the pig lung.

Figure 4–5 Lung tissue from bonnet macaque exposed to 4 MHz diagnostic ultrasound at an MI of 1.8 for 10 min (5 min cranial plus 5 min caudal lung lobe exposures). Note multiple hemorrhagic foci. (Reprinted by permission of Elsevier Science, from Tarantal AF, Canfield DR: Ultrasound-induced lung hemorrhage in the monkey. *Ultrasound Med Biol* 20:65, 1994.)

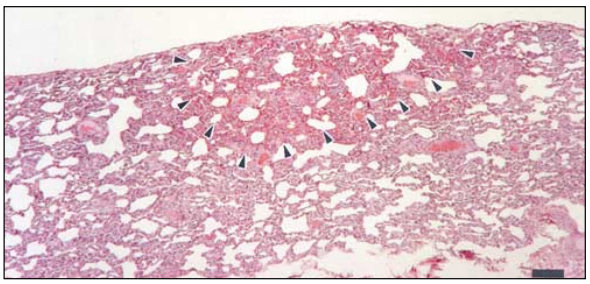

Figure 4–6 Histological appearance of lung tissue from bonnet macaque exposed to 4 MHz pulsed diagnostic ultrasound. Note intra-alveolar hemorrhage (*arrowheads*). Bar scale = 0.2 mm. (Reprinted by permission of Elsevier Science, from Tarantal AF, Canfield DR: Ultrasound-induced lung hemorrhage in the monkey. *Ultrasound Med Biol* 20:65, 1994.)

Figure 4–7 Threshold of ultrasound-induced damage in mouse, rat, and pig lung as a function of center frequency.

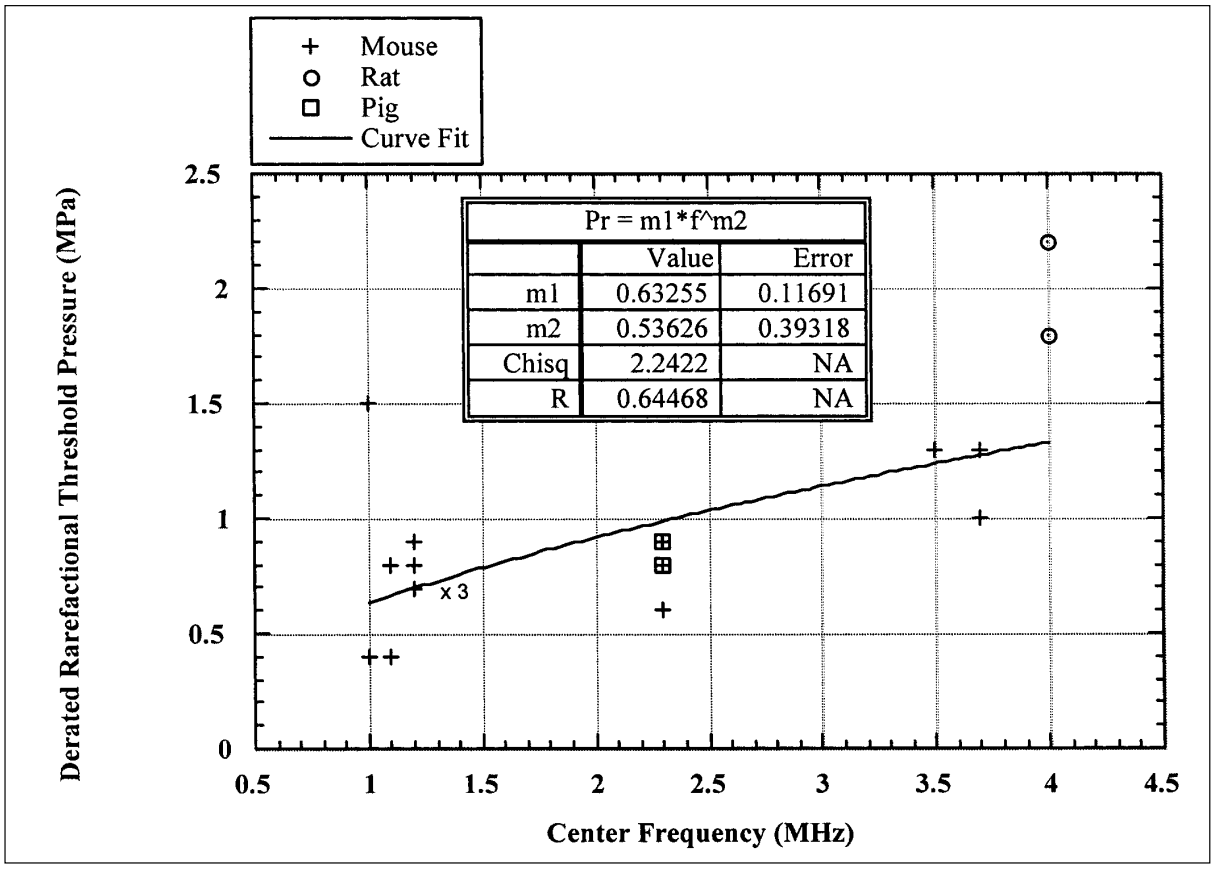

In contrast, the lungs of six adult pigs were exposed to the output of a clinical diagnostic ultrasound scanner with 3 and 6 MHz center frequencies at MI exposure levels between 1.9 and 2.3 in another study (O'Brien and Zachary, 1997). These *in situ* MI values at the pleural surface were estimated by applying a 1 dB/cm-MHz deration to peak rarefactional pressures measured in water (corresponding to 1.8 to 2.2 MPa). Some of the exposure levels utilized in this study exceeded the current limit allowable by the Food and Drug Administration (FDA) for clinical examinations. None of the six pig lungs exhibited any observable damage. Forty-seven adult male rabbits and three mice were also exposed to pulsed ultrasound with 3 and 6 MHz center frequencies over a range of exposure levels. As in the pig, the MI values at the pleural surface of the rabbit were estimated by applying a 1 dB/cm-MHz deration to peak rarefactional pressures measured in water (corresponding to 1.0 to 3.4 MPa). Output levels that clearly produced lung damage in rabbits did not have an adverse effect on pig lungs. Likewise, the three mouse exposures produced greater lung damage than comparable rabbit exposures. Thus, a species-dependent effect was observed in these pulsed ultrasound studies.

4.3.3 Age-Dependent Effects

Results of studies with nonhuman primates (Tarantal and Canfield, 1994) suggested that animals ranging in age from 3 months to 5 years (mean age of 2.5 yr) had a greater propensity for the occurrence of multiple, well-demarcated, circular hemorrhagic foci (0.1–1.0 cm) after exposure to a clinical scanner under maximum output (5 MHz scanned imaging pulses interleaved with 4 MHz pulsed and color Doppler at an MI of 1.8), as compared with older animals (up to 16 yr). These authors proposed that neonates and infants were most likely more susceptible to the effects of exposure because of age-dependent features. However, it was not possible to produce lung damage in 10 to 12 week old crossbred pigs even at MI values as high as 2.1 (O'Brien and Zachary, 1997).

Studies of neonatal swine (Baggs et al, 1996) and of young swine (Dalecki et al, 1997c) indicate that the threshold for lung hemorrhage is not dependent on age within a time frame of 10 d. A similar study in the mouse (Dalecki et al, 1997a) also suggested an age-independent lung-damage threshold for animals ranging in age from 24 hr to 10 wk. But at suprathreshold exposure levels, these researchers observed a greater extent of damage in older animals compared with the younger mice. These findings may be related to the size of the experimental animals rather than age. Note that in young mice, age and size are correlated.

Due to the developmental state of human infants born prematurely, it is possible that certain structural features might make them more susceptible to ultrasound-induced bioeffects. These features include the relative thickness of skin, muscle, fat, connective tissue, and pleura, as well as overall lung maturity, which could increase the risk of lung damage by ultrasound. This is a reasonable concern because ultrasound imaging is frequently used for cardiac applications (echocardiography) in order to diagnose complications of prematurity, such as patent ductus arteriosus and pulmonary artery hypertension. Further data are needed in relevant animal models to address this important issue.

4.3.4 Morphological Observations

Morphological studies describing the microscopic lesions induced by pulsed ultrasound in lung tissue have been documented in monkeys (Tarantal and Canfield, 1994), mice (Penney et al, 1993; Zachary and O'Brien, 1995), rabbits (Zachary and O'Brien, 1995), and in neonatal pigs (Baggs et al, 1996). Studies using juvenile to adult pigs demonstrated that pulmonary hemorrhage could not be induced following exposure to pulsed ultrasound at MI levels as high as 2.1 (Zachary and O'Brien, 1995). In all affected species, lesions were similar and characterized by alveolar hemorrhage and congestion of alveolar capillaries. Lesions in mice and rabbits, and generally in monkeys, were contiguous with the visceral pleural surface of the lung and thus appeared to arise at this site and spread centrally into lung parenchyma (Tarantal and Canfield, 1994; Zachary and O'Brien, 1995). Morphological evaluations of affected lung tissue indicate that pulmonary hemorrhage does not appear to arise from damage to arterioles, venules, respiratory bronchioles, or distal airways. An ultrastructural evaluation by Penney et al (1993) suggested that there was a direct effect of pulsed ultrasound on capillary endothelial and alveolar epithelial cells that was lytic in nature; however, the site of vascular damage could not be identified. Overall, evaluation of both light and electron microscopic studies suggested that lung lesions appeared to originate from the microvascular system located within alveolar septa at the level of the blood-gas barrier and that further investigation was warranted.

The gross organization and cellular composition of the lung is similar in mammals, although there are significant physiological and anatomical differences related to organization of the distal airways, alveolar morphology, and blood supply (Tyler and Julian, 1992). Although the numbers of alveoli within the lung acinus (tissue distal to the terminal bronchioles) are relatively constant among species, there is a distinct difference in the structure and arrangement of the bronchioles supplying the gas-exchange area including the type of terminal bronchioles and extent of smooth muscle incorporated along the length of the alveolar ducts (Mercer and Crapo, 1992). For human and nonhuman primates, smooth muscle fibers extend along the terminal generations of the alveolar ducts, whereas in the mouse, these fibers do not extend past the bronchiole-alveolar duct junction. This finding may suggest that there is a greater potential for hemorrhage and tissue destruction in the mouse lung, particularly where the terminal airways are shorter, thinner, and perhaps less distensible (Tarantal and Canfield, 1994).

Morphological studies demonstrate that capillaries within the alveolar septa of most mammals are arranged as a single layer separated from the air spaces by a thin cellular barrier. The thickness of the alveolar epithelium plus the capillary endothelium is about 100 nm. It is plausible that these regions are more susceptible to conditions under which bubble oscillation and rupture may occur, with a greater degree of damage possible when lung tissues have less ability to expand. Due to this anatomical configuration, Tarantal and Canfield (1994) hypothesized that these regions are more susceptible to conditions under which bubble oscillation and rupture may occur. These authors also noted that an important factor specific to the lung may be the monolayer of surfactant within the alveoli. Surfactant, the fluid lining the alveoli, is responsible for modifying surface tension in order to promote lung expansion and prevent lung collapse (Hawgood and Shiffer, 1991). It is possible that, during exposure to ultrasound, small microbubbles are created within the edges of the surfactant-rich alveolus (location of Type II alveolar epithelial cells). These microbubbles may oscillate and collapse, causing localized disruption of the epithelial-endothelial barrier and subsequent extravasation of red blood cells into the alveolar space. Holland and Apfel (1989; 1990) have previously shown a direct correlation between a reduction in the cavitation threshold and reduced host fluid surface tension. Surfactant therapy administered to premature infants with respiratory distress syndrome could potentially exacerbate cavitation-mediated damage in lungs if they were exposed to high levels of ultrasound (Tarantal, unpublished). Therefore the effect of such exogenous surfactants on ultrasound-induced lung damage is of particular importance.

Physiological properties of lung of various animal species are shown in Section 3, Table 3–1. The critical structural features that can be used to separate species into distinct groups, shown in Section 3, Table 3–2, are pleural thickness (thin versus thick), pleural blood supply (pulmonary artery versus bronchial artery), septal or interlobular connective tissue (scant versus abundant), and relative thickness of the chest wall (thin or thick), which refers to the relative amounts of skin, muscle, fat, and connective tissue. There are significant interspecies structural differences of the lungs, even when lungs and associated structures are evaluated at a subgross level (Plopper and Pinkerton, 1992). While all common mammalian species have parietal and visceral pleural surfaces, the thickness, vascularity, and organization of the mesothelium, submesothelial connective tissue, and vascular system forming, in particular, the visceral pleura, vary among species, as do the extent and distribution of secondary septation with the lung and the distribution of connective tissue elements (Tyler and Julian, 1992). In addition, the source of arterial blood to the visceral pleura varies among species (shown in Section 3, Table 3–2), and this distribution is linked to the thinness or thickness of the visceral pleura. On the basis of these comparisons, human beings clearly can be grouped with pigs (the “thick” group). Therefore, pigs are an important animal model for assessing potential lung injury in human beings in order to understand the pathogenesis of ultrasound-induced lung damage and hemorrhage, as well as the physiological implications. The group that possesses a “thin” visceral pleura includes rats and rabbits. The animals in the "thin" group serve as a critical structural biological control group to test the hypothesis that structural differences are important components when considering the potential for damage in humans. More research is necessary to establish a correlation of the thinness of the visceral pleura and the potential for lung damage.

4.3.5 MI versus Intensity as a Better Indicator of Mechanical Bioeffect Risk

O’Brien and Zachary (1997) compared the performance of the MI (Apfel and Holland, 1991; AIUM / NEMA, 1992b) to the derated spatial peak, pulse average intensity ($I_{SPPA.3}$) in tracking ultra-

sound-induced lung hemorrhage in a rabbit model. The principal consideration of the study was to assess experimentally the question: "Is the MI an equivalent or better indicator of nonthermal bioeffect risk than $I_{SPPA.3}$?" This question was motivated by the adoption of the MI in place of $I_{SPPA.3}$ as the acoustic output quantity regulated by the FDA (1994). Currently, the maximum allowed limit for the MI is 1.9. Forty-seven adult New Zealand white male rabbits were exposed to a range of ultrasound amplitudes at center frequencies of 3 and 6 MHz for 5 min. A calibrated, commercial diagnostic ultrasound system was used as the source with output levels exceeding, in some cases, permissible FDA levels. The MI was shown to be at least an equivalent, and in some cases a better, indicator of rabbit lung damage than either the $I_{SPPA.3}$ or derated peak rarefactional pressure. The assessment of the correlation of MI with a bioeffect such as lung hemorrhage is needed over a greater frequency range (e.g., 2 to 10 MHz) to determine clinical relevance.

4.3.6 Detection of Inertial Cavitation *In Vivo*

The high amplitude shock waves employed in ESWL can generate cavitation in animal tissues (Delius et al, 1990; Coleman et al, 1992; Huber et al 1994). The physical evidence that cavitation also occurs in human tissue during routine clinical ESWL comes from the appearance of well-defined hyperechoic regions in ultrasound images during therapy that are attributed to scatter from newly generated bubbles. In addition, Coleman et al (1996) have employed a 1 MHz, focused piezoceramic hydrophone, first described by Coakley (1970), to monitor the 1 MHz component of the broadband acoustic emission that accompanies bubble dynamics induced by ESWL. This evidence indicates that the acoustic emission arises from inertial cavitation in human tissue during clinical application of ESWL.

Although a proven phenomenon *in vitro* (Holland et al, 1992), the occurrence of cavitation *in vivo* due to diagnostic ultrasound has been difficult to document in mammalian systems primarily due to the transient nature of its occurrence (i.e., on a μs time scale) and the localized character of the resultant effects (i.e., < 10 μm). To explore the hypothesis of cavitation-based bioeffects from diagnostic ultrasound, Holland et al (1996) determined the thresholds of damage in rat lungs exposed to 4.0 MHz pulsed Doppler and color Doppler ultrasound. In this study, a 30 MHz acoustic detection scheme developed by Roy et al (1990) was employed to provide the first direct evidence of cavitation from diagnostic ultrasound pulses. Damage was observed with histological features consistent with those seen in mice and monkeys due to diagnostic ultrasound exposures. However, in this limited study, bubble activity was not correlated with histological damage. The question remains: Does cavitation, if produced by diagnostic ultrasound *in vivo*, cause significant biological effects?

4.3.7 *In Vivo* Effects in Mice Exposed to 30 kHz Continuous Wave Ultrasound

Studies have been performed under continuous-wave (CW) conditions at 30 kHz using mice (O'Brien and Zachary, 1994b) with the goal of assessing the frequency dependence of the threshold pressure levels as compared with those reported under pulsed wave (PW) conditions at 1 to 4 MHz by Child et al (1990). The acoustic pressure threshold levels necessary to produce mouse lung damage *in vivo* were evaluated to assess the safety of a commercial, whole-body ultrasound cleaner for geriatric patients in a bathtub environment. The same mouse strain and anesthetic agents were used in both experimental protocols. The photos in Figures 4–8 through 4–10 demonstrate the typical features of a sham-exposed control and CW ultrasound-induced lung damage in the mouse with comparative histological sections.

Linear regression analysis of lung damage scores versus exposure acoustic pressure levels yielded highly significant regressions with slightly increasing slopes and non-zero intercepts as exposure duration increased. The acoustic pressure threshold for lung damage was between 80 and 100 kPa at 30 kHz, or $p/\sqrt{f}$ values between 0.46 and 0.58, where p is the acoustic pressure threshold in MPa and f is the ultrasound frequency in MHz (O'Brien and Zachary, 1994b). It is important to note that this quantity is similar to the MI, which is equal to $p_{r.3}/\sqrt{f}$, where $p_{r.3}$ is the peak rarefactional pressure that has been derated by 0.3 dB $cm^{-1}MHz^{-1}$ at the location of the maximum pulse intensity integral, and f is the center frequency in MHz. The results of Child et al (1990) from experiments conducted between 1.1 and 3.7 MHz yielded $p/\sqrt{f}$ values between 0.4 and 0.7, thus suggesting a $\sqrt{f}$ frequency dependency for ultrasound-induced lung damage for the mouse.

Lung damage produced by 30 kHz CW ultrasound did not appear to be a strong function of exposure duration (O'Brien and Zachary, 1994b). In general, these findings showed that the mechanism leading to hemorrhage occurred early (within the first 5 min) in the exposure period. As sonication

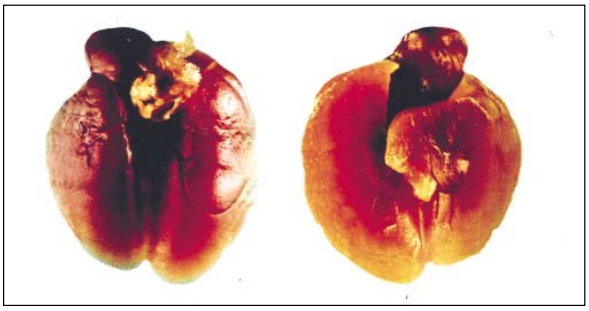

Figure 4–8 Sham-exposed control mouse lung exhibiting no lesions (fixed tissue). Left: dorsal-ventral view. Right: ventral-dorsal view. (Photo courtesy of James F. Zachary, DVM, PhD.)

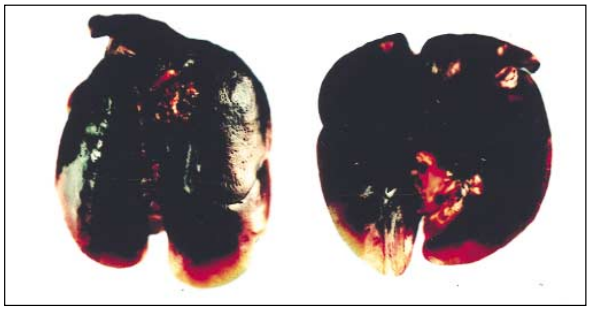

Figure 4–9 Mouse lung exposed to 30 kHz, CW ultrasound for 5 min exhibiting severe diffuse intraparenchymal hemorrhage (fixed tissue). Left: dorsal-ventral view. Right: ventral-dorsal view. (Reprinted by permission of Elsevier Science, from O'Brien WD Jr., Zachary JF: Mouse lung damage from exposure to 30 kHz ultrasound. *Ultrasound Med Biol* 20:287, 1994b.)

progressed, the degree of lung damage only increased slightly. The mechanisms responsible for the damage from the 30 kHz CW ultrasound and 1–4 MHz pulsed diagnostic ultrasound could be different. Further research is necessary to determine the mechanism(s) of ultrasound-induced damage in lung in animals exposed to either pulsed or CW ultrasound. Therefore, caution should be made when interpreting the 30 kHz results within the pulsed diagnostic ultrasound context.

4.3.8 Species-Dependent Effects Due to 30 kHz CW Exposures

Lung damage in mice, rabbits, and pigs was studied at 30 kHz under CW conditions (O'Brien and Zachary, 1994a, 1994b, 1996). Suprathreshold exposure levels were utilized to compare the extent of hemorrhage in pigs and rabbits to the mouse. The study design did not determine threshold levels. O'Brien and Zachary (1994a) also evaluated the hypothesis that the mouse may not be a suitable animal model for studies that examine ultrasound-induced effects on lung tissue for purposes of extrapolating or estimating the degree of potential damage in other large mammalian species, particularly the human. To test this hypothesis, the rabbit was selected for comparison to the mouse because the rabbit exhibits sufficient physiological and morphological differences from the mouse. Extensive lung hemorrhage and death occurred in the mouse at 100 and 145 kPa, whereas considerably less hemorrhage was noted for the rabbit and even less hemorrhage for the pig. Neither rabbits nor pigs were killed due to lung injury following exposure of the lung to ultrasound at similar exposure levels.

A clear difference between mouse and rabbit sensitivities to lung damage at each of the exposure pressure levels was observed, with the rabbit being

Figure 4–10 Left: Sham exposed control mouse lung (low magnification) exhibiting no lesions (H&E stain). Center: Mouse lung exposed to 30 kHz, CW ultrasound for 5 min (low magnification). Alveoli are contiguous with the visceral pleura and are filled with blood. The hemorrhage spreads to a finite limit into adjacent lung parenchyma (H&E stain). Right: CW exposed mouse lung (high magnification) exhibiting alveolar hemorrhage (H&E stain). The visceral pleura and contiguous alveolar septa are intact. (Photo courtesy of James F. Zachary, DVM, PhD.)

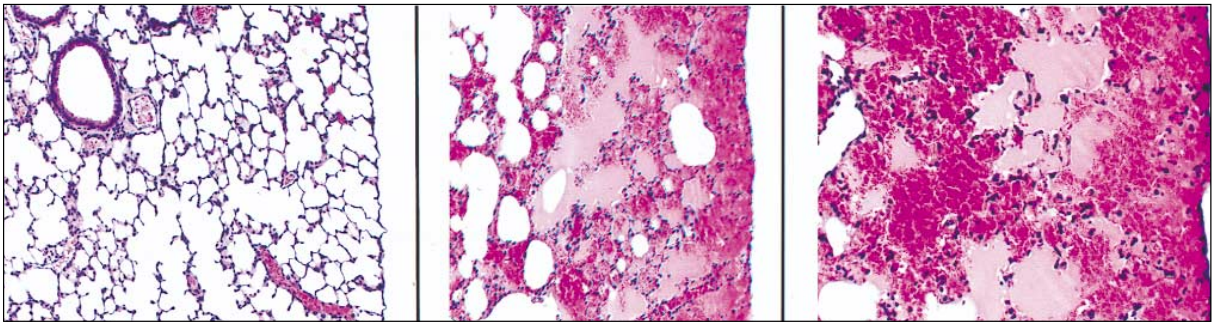

much less sensitive to damage than the mouse (O'Brien and Zachary, 1994a). In this study, the lung damage score, which increased with the amount of lung damage, was plotted against the insonifying peak rarefactional pressure. Linear regression analyses of the lung damage scores versus acoustic pressure exposure levels for the two species were also performed. Both regressions were highly significant ($P < 0.0001$ and $P = 0.009$, respectively) with a much greater slope for mice compared with that for rabbits by a factor of 3.6 (0.069 / 0.019), demonstrating a difference in degree of sensitivity to lung damage between these two species.

This study was extended to pigs to explore the species dependence of the degree of sensitivity to ultrasound-induced lung damage at an ultrasonic frequency of 30 kHz under CW exposure conditions (O'Brien and Zachary, 1996). Eighteen mice were used as positive controls (10 min duration at 145 kPa). Because pig lung has numerous physiological and anatomical similarities to human lung, it was selected as the animal model for these studies. Linear regression analyses of lung damage scores versus acoustic pressure levels for the two species, rabbit and pig, were performed. Both regressions were highly significant (both $P < 0.0001$) with a much greater slope for rabbits compared with pigs by a factor of 3.8 (0.0069 / 0.0018) demonstrating the difference in degree of sensitivity to lung damage between these two species.

The mean and standard deviation for the combined (by species) lung damage scores for 43 mice, 22 rabbits, and 16 pigs from all three studies at an acoustic pressure level of 145 kPa and an exposure duration of 10 min (see Fig. 4–11) suggest that ultrasound-induced lung damage is a strong function of species (O'Brien and Zachary, 1994a, 1994b, 1996). Also, linear regression analyses of lung damage scores versus all of the acoustic pressure levels for the three species from all three studies were performed. All three of these regressions were highly significant (all $P < 0.0001$) with a much greater slope for mice compared with rabbits by a factor of 3.9 (0.026 / 0.0066), with a much greater slope for rabbits compared with pigs by a factor of 3.7 (0.0066 / 0.0018), and with a much greater slope for mice compared with pigs by a factor of 14.4 (0.026 / 0.0018), demonstrating the difference of sensitivity to lung damage among these three species, in the order mouse > rabbit > pig.

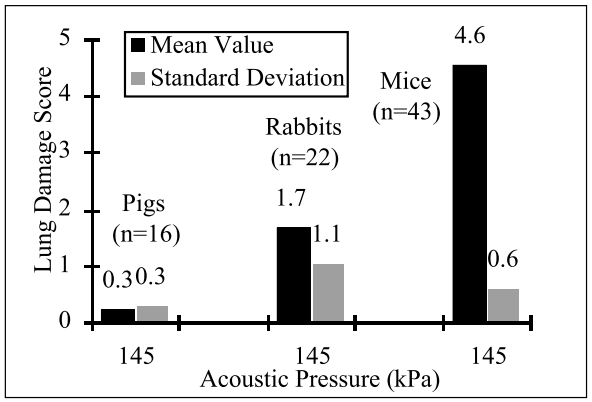

Figure 4–11 Lung damage score at an acoustic pressure amplitude of 145 kPa for mice, rabbits, and pigs exposed to 30 kHz continuous wave ultrasound. (Adapted from and reprinted by permission of Elsevier Science, from O'Brien WD Jr., Zachary JF: Comparison of mouse and rabbit lung damage exposure to 30 kHz ultrasound. Ultrasound Med Biol 20:299, 1994a; and O'Brien WD Jr., Zachary JF: Mouse lung damage from exposure to 30 kHz ultrasound. Ultrasound Med Biol 20:287, 1994b; and O'Brien WD Jr., Zachary JF: Rabbit and pig lung damage from exposure to CW 30-kHz ultrasound. *Ultrasound Med Biol* 22:345, 1996.)

4.4 Clinical Implications of Lung Damage

Humans and animals that suffer trauma to the lungs or pulmonary hemorrhage can exhibit abnormalities of pulmonary function (Prentice and Ahrens, 1994; Kirton et al, 1995). The degree of abnormal function is dependent upon the severity of injury and the proportion of total lung volume damaged. Because of the very large reserve volume of the lungs, which is only required during exhaustive exercise, patients can accommodate rather severe lung damage and still survive. There exists abundant peer-reviewed published scientific literature that clearly and convincingly documents that ultrasound at commercial diagnostic levels can produce lung damage and focal hemorrhage in a variety of mammalian species (see Table 4–1). The degree to which this is a clinically significant problem in humans is not known.

Given the thresholds for lung hemorrhage in laboratory animals, what can be inferred about the sensitivity of human lung to diagnostic ultrasound? It is unlikely that an ethically acceptable protocol can be devised that will directly determine the threshold for hemorrhage in human subjects. On the one hand, the observations by Meltzer and colleagues (1998) suggest that human lung is not markedly more susceptible to ultrasound exposure than that of animals that have been used in systematic threshold determinations. On the other hand, in view of the thresholds for damage in various laboratory animals, it would not be responsible to assume that the threshold for hemorrhage in human lung was significantly lower.

4.5 ULTRASOUND-INDUCED EFFECTS ON INTESTINE

In addition to effects in the lung, ultrasonically induced petechial hemorrhage has also been observed in the mouse intestine. Lehmann and Herrick (1953) reported the production of petechial hemorrhage in the abdomen of mice exposed to 1 MHz therapeutic ultrasound. Typical therapeutic exposures involved unfocused transducers generating CW or long burst-mode ultrasound at spatial peak intensities of a few watts/cm^2. The mechanism of damage was attributed to cavitation by these authors because the damage appeared to be mechanical upon histological examination. Intestinal hemorrhage has also been reported in rats due to therapeutic ultrasound exposure (Cowden and Abell, 1963). Because of the long pulse durations utilized in therapeutic ultrasound exposures, heating as a mechanism for damage cannot be ruled out. Indeed, some investigators (Miller DL and Thomas, 1994) observed both hyperemia and petechial hemorrhage in mouse intestine exposed to 1.0 MHz pulsed and CW ultrasound. Pulsed exposure conditions included a 1 ms pulse duration and 250 or 500 Hz PRFs. Histologically, the petechiae appeared to be localized mostly to the lamina propria of the mucosa. In addition, both hyperemia and petechial hemorrhage were observed in mouse intestine exposed to local heating from radio-frequency diathermy at 10.35 MHz. Therefore, these authors (Miller DL and Thomas, 1994) concluded that the ultrasonically induced petechiae appeared to be attributable to heating and not cavitation.

Petechial hemorrhage can be attributed unambiguously to mechanical mechanisms from exposure to ESWL. The relatively low 1-Hz PRF yields low time-average intensities and no significant heating. Petechial hemorrhage from lithotripter shockwaves has been produced in rat intestine (Chaussy, 1982) and mouse intestine (Raeman et al, 1994; Miller DL and Thomas 1995a; Dalecki et al, 1995c). Hemorrhage has also been observed in liver and kidney from lithotripter shockwaves (Chaussy, 1982; Delius et al, 1988b, 1990), but not from pulsed diagnostic ultrasound in these organs (Carstensen et al, 1990b). As evidence for cavitation involvement in the damage, lithotripter shock waves generate hyperechoic regions attributed to bubbles, which are observed on ultrasonic images (Kuwahara et al, 1989; Delius et al, 1990). In addition, mechanical inversion of the lithotripter shockwave via the use of a novel pressure release reflector inhibits the formation of cavitation and simultaneously decreases the effectiveness in renal calculi destruction (Bailey et al, 1998).

One group (Miller DL and Thomas, 1995a) observed that the number of intestinal lesions increased with increasing number of shockwaves and with increasing amplitude. The threshold for intestinal damage in the mouse was roughly between 1.6 and 4.0 MPa peak positive pressure and between 1.4 and 3.5 MPa peak negative pressure. Dalecki et al (1995c) also observed that the extent of intestinal damage in the mouse increased with the output level of the lithotripter once the threshold level was exceeded. In another study in mice, Dalecki et al (1996) demonstrated that the presence of gas in the intestine vastly increased the potential for intestinal hemorrhage. Pregnant mice were exposed to lithotripter shockwaves with 10 MPa peak positive and 2.5 MPa peak rarefactional pressure amplitudes. All maternal intestines showed hemorrhagic regions extending several centimeters in length. In contrast, the exposed fetuses exhibited minimal intestinal hemorrhage. The results of these authors support a bubble activation or cavitation mechanism for the production of intestinal hemorrhage by exposure to acoustic fields.

Thresholds for damage in the mouse intestine due to diagnostic pulses of ultrasound have also been explored (Dalecki et al, 1995b). Pulses with a duration of 10 μs and a PRF of 100 Hz at center frequencies of 0.7, 1.1, 2.4, and 3.6 MHz yielded thresholds for intestinal hemorrhage listed in Table 4–2. The tabulated $p/\sqrt{f}$ values were calculated by utilizing insertion loss measurements of Dalecki et al (1995b) rather than derating the peak rarefactional pressure by 0.3 dB/cm-MHz. Thermocouple measurements of the temperature rise during ultrasound exposure revealed temperature elevations of 2°C or less even at the highest exposure levels. Near the threshold, heating was much less and clearly too small to support a thermal mechanism for damage. The frequency dependence of the production of intestinal hemorrhage is consistent with a cavitational, or gas body activation, mechanism of damage.

Table 4–2: Thresholds for Murine Intestinal Hemorrhage as a Function of Frequency[a]

Frequency (MHz)	Threshold Levels p_+ (MPa)	p_- (MPa)	I_{SPPA} (W/cm^2)	$p/\sqrt{f}$
0.7	0.9	0.9	16	1.1
1.1	1.3	1.5	57	1.4
2.4	11.5	3.9	1075	2.5
3.6	7.8	2.8	505	1.5

[a]Dalecki et al (1995b).